Understanding the deposition and reaction mechanism of ammonium bisulfate on a vanadia SCR catalyst: A combined DFT and experimental study

Xiangmin Wang[a,b], Xuesen Du[a,b,*], Shaojun Liu[c], Guangpeng Yang[a,b], Yanrong Chen[a,b], Li Zhang[a,b], Xin Tu[d,*]

[a] Key Laboratory of Low-grade Energy Utilization Technologies and Systems, Ministry of Education, Chongqing University, Chongqing, 400044, China

[b] School of Energy and Power Engineering, Chongqing University, Chongqing, 400044, China

[c] School of Energy and Power, Jiangsu University of Science and Technology, No.2 Mengxi Road, Zhenjiang, Jiangsu 212003, China

[d] Department of Electrical Engineering and Electronics, University of Liverpool, Liverpool L69 3GJ, UK

*Corresponding authors:

Dr. Xuesen Du, xuesendu@cqu.edu.cn ;

Dr. Xin Tu, xin.tu@liverpool.ac.uk

Abstract: The deactivation of NH_3-selective catalytic reduction (SCR) catalysts due to NH_4HSO_4 deposition at low temperatures (< 300 ^oC) is still a significant challenge. In this work, we present a comprehensive mechanism describing the formation, deposition, and reaction of NH_4HSO_4 on a V_2O_5/TiO_2 catalyst using a combination of theoretical and experimental methods. The results show that NH_4HSO_4 is mainly formed in the gas phase through the nucleation of SO_3, H_2O, and NH_3 and then deposits onto the catalyst surface. The decomposition of NH_4HSO_4 on the surface of the V_2O_5/TiO_2 catalyst consists of two steps: NO is reduced by the NH_4^+ of NH_4HSO_4 forming N_2 and H_2O by transferring an electron to the adjacent vanadium site, followed by a reoxidation of the reduced vanadium site by either O_2 or NO_2. At low temperatures, due to the weak reoxidizing ability of O_2, the reaction of NH_4HSO_4 with NO in the NO/O_2 mixture is rather slow. Adding NO_2 can remarkably enhance the decomposition of NH_4HSO_4 on the catalyst surface. Our results reveal that the rate-determining step of the reaction between NH_4HSO_4 and NO/O_2 is the reoxidation of the reduced vanadium site and that NO_2 is a better reoxidizing agent than O_2, which has been confirmed by X-ray photoelectron spectroscopy analysis and the designed transient response method experiments. Finally, the catalyst sulfur tolerance test has proven that the commercial V_2O_5-WO_3/TiO_2 catalyst can successfully maintain its long-term activity for NO_x reduction in SO_2-contained flue gas at 250 ^oC due to the rapid decomposition of deposited NH_4HSO_4 on the catalyst surface by the NO/NO_2 mixture.

Keywords: Selective catalytic reduction; NH_4HSO_4 deposition; V_2O_5/TiO_2; NO_2; Density functional theory

1. Introduction

Nitrogen oxides NO_x (NO and NO_2) emitted from stationary and mobile sources are a significant contributor to the formation of multiple environmental pollutants (i.e., acid rain, smog, and haze). The selective catalytic reduction (SCR) of NO_x with NH_3 is the most common technology used to control NO_x emissions [1, 2]. In recent years, low-temperature SCR technology has attracted increasing attention because of its potential capacity to reduce the NO_x emission from load-following power plants and other stationary sources (e.g., the metallurgical industry and chemical processes) [3-5]. Correspondingly, a large number of catalysts with excellent low-temperature activity have been designed and developed for low-temperature SCR processes, such as MnO_x-TiO_2 [6-9], Cu-TiO_2 [10, 11] and Cu-zeolites [12-16]. However, SO_3 (either contained in flue gas or oxidized from SO_2 by SCR catalysts [17-20]), is a highly reactive acid gas [21], which can react efficiently with NH_3 and H_2O in SCR processes and results in the formation of unfavorable by-products such as ammonium sulfate and bisulfate [18, 22-27]. In particular, ammonium bisulfate (NH_4HSO_4) is sticky and corrosive and can be deposited on the surface of SCR catalysts, resulting in their deactivation [13, 28-44], which limits the use of the low-temperature SCR technology on a commercial scale.

To develop an efficient low-temperature SCR process for the treatment of SO_2-containing flue gas, considerable efforts have been dedicated to understanding the decomposition and reaction behaviors of NH_4HSO_4 on the surfaces of SCR catalysts. Ye et al. and Song et al. [31, 45] found that introducing CeO_2 or WO_3 to a V_2O_5/TiO_2 catalyst could promote the decomposition of deposited NH_4HSO_4 on the catalyst surface. Pang et al. [46] used thermogravimetry to investigate the thermal decomposition of NH_4HSO_4 formed on different

metal oxides. These studies have provided fundamental information that can be used to design low-temperature SCR catalysts with an excellent resistance to NH_4HSO_4 deposition [37, 39, 40, 47]. However, the thermogravimetric analysis of NH_4HSO_4 deposition in these studies used dry air or N_2, which is different to the atmosphere in industrial NH_3-SCR processes.

When looking at removing the deposited NH_4HSO_4, it was shown that the reaction between the deposited NH_4HSO_4 on the catalyst surface and NO_x in flue gas is more effective compared to the pyrolysis of NH_4HSO_4 at the same temperature [28, 29, 33, 34]. Previous studies [28, 29] confirmed that the reaction of NO with the ammonium ions from NH_4HSO_4 accelerates the decomposition of NH_4HSO_4 on the surface of a V_2O_5-WO_3/TiO_2 catalyst. Ye et al. [32] doped Nb_2O_5 and Sb_2O_5 onto a V_2O_5-WO_3/TiO_2 catalyst to accelerate the reaction of deposited NH_4HSO_4 with gaseous NO. One of our previous studies also found that NO_2 could efficiently accelerate the reaction between the deposited NH_4SHO_4 and NO_x at low temperatures [33]. The low-temperature activity of a commercial V_2O_5-WO_3/TiO_2 catalyst can be well-maintained in the presence of SO_2 and H_2O when adding NO_2 to the reaction due to the fast decomposition of the deposited NH_4HSO_4 [34]. We also found that the rapid consumption of NH_4^+ from NH_4HSO_4 inhibited the continuous deposition of NH_4HSO_4 and resulted in an enhanced sulfur tolerance of the catalyst at low temperatures [34]. These results have successfully demonstrated that promoting the reaction of NH_4HSO_4 with NO_x on the catalyst surface is an effective way to improve the sulfur-resistance of the SCR catalysts, which is critical to the commercialization of low-temperature SCR processes.

To further accelerate the decomposition of deposited NH_4HSO_4, considerable efforts have been devoted to understanding the mechanisms of the NH_4HSO_4 deposition and reaction over

SCR catalysts at various temperatures. Li et al. [36] developed a molecular model to investigate the formation and deposition of NH_4HSO_4 over a V_2O_5-WO_3/TiO_2 catalyst and found that a tightly bound sulfate on TiO_2 could react with adjacent ammonium species to form NH_4HSO_4 at low temperatures. This finding is consistent with the results obtained from the model proposed by Phil et al. and Qu et al. [47, 48], based on this model Phil et al. [47] used the quantum chemical calculation to estimate the bonding strength between NH_4HSO_4 and transition metals. Furthermore, in-situ diffuse reflectance infrared Fourier transform spectroscopy (DRIFTS) has been widely used to investigate the reaction of deposited NH_4HSO_4 with NO_x on the surface of various catalysts. It is commonly accepted that the NH_4^+ of NH_4HSO_4 could react with NO_x while the sulfate ion remains on the catalyst surface in the form of a metal sulfate [33, 35, 45, 48]. However, the detailed mechanism of the reaction between NH_4HSO_4 and NO_x, especially on the atomic level, remains unclear. Thus, getting new insights into the reaction mechanism is crucial to better understand the structural changes of the active sites and the critical steps of the reaction between NH_4HSO_4 and NO_x on SCR catalysts, which can provide valuable knowledge to design novel SO_2-resistant catalysts for low-temperature SCR processes.

In this work, the formation and deposition models of NH_4HSO_4 on a V_2O_5/TiO_2 catalyst have been investigated using density functional theory (DFT) modeling combined with a range of catalyst characterization techniques. Temperature-programmed surface reaction (TPSR) and in-situ DRIFTS analysis have been carried out to understand the reactions between NO_x (NO only and NO/NO_2 mixture) and ammonia species (freely absorbed NH_3 and deposited NH_4HSO_4). Furthermore, X-ray photoelectron spectroscopy (XPS) analysis, together with the

designed transient response method experiments, was performed to investigate the effect of NO_2 on the reaction of NH_4HSO_4 with NO_x. The complete reaction mechanisms for these reactions have been proposed and discussed by using the calculation and analysis of the energy diagrams; structures of the active sites and transition states; and the formation of reaction intermediates. Finally, the sulfur tolerance of a commercial V_2O_5-WO_3/TiO_2 catalyst was evaluated in SO_2-containing flue gas at 250 ^oC in an NO_2-containing atmosphere where the deposited NH_4HSO_4 can be rapidly decomposed.

2. Experimental and computational details

2.1 Catalyst preparation

The V_2O_5/TiO_2 sample with 1 wt.% V_2O_5 loading was prepared by the wetness impregnation method, using commercial Degussa P25 TiO_2 as the support. Ammonium vanadate (NH_4VO_3) was dissolved in water, acidified by oxalic acid, and used as the aqueous solution for the impregnation. After impregnation, the prepared samples were dried at 110 ^oC for 12 h and subsequently calcined in a muffle furnace at 500 ^oC for 5 h. The TiO_2 and 1 wt.% V_2O_5/TiO_2 catalysts were named as Ti and VTi, respectively. The 20 wt.% NH_4HSO_4-deposited V_2O_5/TiO_2 sample was prepared by the previously reported impregnation method and was denoted as VTi-p [23, 29]. A V_2O_5-WO_3/TiO_2 catalyst was also prepared using the same preparation method as above for the sulfur tolerance tests. Ammonium metatungstate ($(NH_4)_6H_2W_{12}O_{40}$) was used as the precursor of WO_3. The loadings of V_2O_5 and WO_3 in V_2O_5-WO_3/TiO_2 were 1 wt.% and 5 wt.%, respectively. The V_2O_5-WO_3/TiO_2 catalyst was referred to as VWTi for short. The sulfated VWTi catalyst was prepared through the sulfation of the VWTi catalyst at 250 ^oC for

1 hour and was denoted as VWTi-S. The sulfation atmosphere contained 1000 ppm SO_2, 5 vol.% O_2, and N_2 as balance with a total gas flow rate of 1.5 L/min, corresponding to a gas hourly space velocity (GHSV) of 225000 mL/(g·h).

2.2 Reaction systems

The temperature-programmed surface reaction of NH_4HSO_4 with NO_x on the V_2O_5/TiO_2 catalyst (0.4 g) was carried out in a quartz tube reactor. The feed gas mixture contained 500 ppm NO (or 250 ppm NO and 250 ppm NO_2), 5 vol.% O_2, 10 vol.% H_2O and N_2 as balance with a total gas flow rate of 1 L/min, corresponding to a GHSV of 150000 mL/(g·h). The temperature was ramped up from 100 ^oC to 450 ^oC at a heating rate of 5 ^oC/min. The reaction conditions for the testing of the SCR catalysts were as follows: 500 ppm NO, 500 ppm NH_3, 5 vol.% O_2, 10 vol. % H_2O and N_2 as balance with the same total gas flow rate (1 L/min) and GHSV. The outlet concentration of NO, NO_2, N_2O, and NH_3 in the flue gas was analyzed by a Protea ProtIR 204M online infrared gas analyzer. The conversion of NO_x can be calculated by:

$$\mathrm{NO}_x \text{ conversion } (\%) = \frac{[\mathrm{NO}_x]_{in} - [\mathrm{NO}_x]_{out}}{[\mathrm{NO}_x]_{in}} \times 100 \quad (1)$$

The selectivity of N_2 is defined as

$$\mathrm{N}_2 \text{ selectivity } (\%) = \left(\frac{[\mathrm{NO}_x]_{in} + [\mathrm{NH}_3]_{in} - [\mathrm{NH}_3]_{out} - [\mathrm{NO}_x]_{out} - 2[\mathrm{N}_2\mathrm{O}]_{out}}{[\mathrm{NH}_3]_{in} + [\mathrm{NO}_x]_{in} - [\mathrm{NH}_3]_{out} - [\mathrm{NO}_x]_{out}} \right) \times 100 \quad (2)$$

The reoxidation of the reduced VTi-p catalyst with different oxidizing agents (O_2 and NO_2) was investigated using a transient response method (TRM). 0.4 g of the VTi-p sample was placed in a fixed bed reactor. The catalyst was firstly reduced in the presence of NO at 250 ^oC

until no NO was consumed, which indicates that all the reactive V^{5+} ions on the catalyst have been reduced to V^{4+}. Then, the reduced catalyst was treated at the same temperature with different oxidizing agents (O_2 and NO_2). The VTi-p catalyst underwent several reduction-oxidation cycles under the above experimental conditions until the NH_4HSO_4 on the catalyst surface was entirely decomposed by NO. For comparison data was also collected without a catalyst present for all experiments.

The activities of the VWTi and VWTi-S catalysts were evaluated in both the standard SCR and fast SCR reactions. 0.4 g catalyst was used in these experiments with a total feed flow rate of 1.5 L/min and a GHSV of 225000 mL/(g·h). The feed gas composition of the standard SCR reaction consisted of 500 ppm NO, 500 ppm NH_3, 5 vol.% O_2 and N_2 as balance, while the feed gas in the fast SCR reaction contained 250 ppm NO, 250 ppm NO_2, 500 ppm NH_3, 5% O_2 and N_2 as balance. The sulfur tolerance of the VWTi catalyst in the standard and fast SCR reactions was also investigated at a reaction temperature of 250 ^oC and a GSHV of 150000 mL/(g·h). The effect of SO_2 (1000 ppm) and H_2O (10 vol.%) on the stability of the VWTi catalyst was evaluated.

2.3 Catalyst characterization

The surface morphology of the catalysts was measured using a TESCN VEGA 3 SBH scanning electron microscope. The scanning electron microscope (SEM) images were obtained from secondary electrons using an accelerating voltage of 3 kV.

The Fourier transform infrared (FTIR) spectra ranging from 4000 cm^{-1} to 400 cm^{-1} with a resolution of 4 cm^{-1} were collected using a Nicolet IS10 FTIR spectrometer at ambient pressure.

The samples were treated with the KBr pellet method before characterization.

XPS experiments were carried out on a Thermo Scientific Escalab 250Xi spectrometer with a monochromatized Al Kα line. The binding energies of the series of photoelectron peaks were corrected by using the C 1s peak at 284.5 eV as the standard.

Nitrogen adsorption and desorption of the samples was performed using an ASAP 2460 apparatus at -196°C. The tested samples were degassed at 200 ^{o}C for six hours prior to the N_2 adsorption. The surface area of the catalysts was determined by the Brunauer-Emmett-Teller (BET) method.

In-situ DRIFTS analysis was carried out using a Nicolet Nexus 6700 FTIR spectrometer with an MCT/A detector. A background spectrum in an N_2 flow was sampled before each experiment. All the IR spectra were obtained by collecting 64 scans with a resolution of 4 cm^{-1}.

2.4 Computational details

In this study, the formation of NH_4HSO_4, as well as its deposition and reaction on uncovered and vanadium loaded anatase (001) surfaces, was investigated using computational modeling. Both periodical and finite boundary conditions have been considered in the simulation to understand the formation of NH_4HSO_4 in the gas phase. As the deposition and reaction of NH_4HSO_4 occurs on the surfaces of the catalysts, the models of the TiO_2 and V_2O_5/TiO_2 systems contain a large number of atoms; and thus only the periodical boundary condition has been used in the modeling to gain new insights into the deposition and reaction of NH_4HSO_4 on the catalyst surfaces.

All the calculations with periodical boundary conditions were performed using Material Studio 8.0 modeling Dmol3. GGA-PBE was used as the exchange-correlation function [49, 50]. A double numerical basis set with a polarization (DNP) function on all atoms was used throughout the calculations. Core electrons were treated with effective core potentials (ECP), and the global orbital cutoff was 4.5 Å. The convergence criteria for the self-consistent field energy and displacement were 1×10^{-6} Ha and 5×10^{-3} Å, respectively. A Monkhorst-Pack grid of 3×3×1 was chosen to be the number of k-points for the Brillion zone. The parameters of the optimized TiO_2 anatase were calculated to be a = b = 3.81 Å and c = 9.47 Å, deviating from the experimental values by 0.54% and 0.42%, respectively [51]. Afterwards, the (001) surface with four-layer was cut from the optimized (4×3) supercell using a vacuum slab of 15 Å in the z-direction. The cut anatase (001) surface was optimized with only the top layer being relaxed (as shown in Figure 2 (a)). In this study, transition-state searches were performed using synchronous transit methods, including both the Linear Synchronous Transit (LST) and the Quadratic Synchronous Transit (QST) approaches. The low vanadium loading VTi catalyst model was developed with VO_3H bonding on the TiO_2 (001) surface (as shown in Figure 2 (d)), which was validated by Arnarson et al.[52, 53]. The cluster-based calculation of NH_4HSO_4 formation was carried out using the Gaussian 09 module at the B3LYP/6-311++G(D.P) level [54]. In this study, the adsorption energy (ΔE_{ads}) was calculated by:

$$\Delta E_{ads} = E_{total} - (E_{adsorbate} + E_{substrate})$$

3. Results and discussion

3.1 Formation of NH_4HSO_4 and its deposition on an SCR catalyst

H_2SO_4 is a crucial intermediate in the formation of NH_4HSO_4 in NH_3-SCR processes. NH_4HSO_4 can be produced through the neutralization of H_2SO_4 with NH_3, while H_2SO_4 is initially formed via the reaction of SO_3 with H_2O. However, we found that it was difficult to oxidize SO_2 to SO_3 over a VTi catalyst at low temperatures when using a low vanadium loading [17, 55]. In industrial-scale NH_3-SCR processes, the initial concentration of SO_3 ($\approx$1% of SO_x is SO_3) in the flue gas is much higher than the SO_3 concentration produced via SO_2 oxidation on a catalyst [26, 27]. SO_3 can easily react with NH_3 and H_2O to form NH_4HSO_4 in the gas phase, which then deposits on the surface of the SCR catalyst.

As shown in Figure 1, two different mechanisms of NH_4HSO_4 formation were calculated using both the hybrid function (cluster) and PBE (periodical boundary) methods. In the H_2SO_4-NH_3 reaction mechanism (shown in Figure 1 (a) and (b)), the formation of H_2SO_4 via the reaction of SO_3 with H_2O is the rate-determining step. The energy profiles calculated from the cluster and periodical models show that the energy barrier of the H_2SO_4 formation was 1.25 eV and 1.01 eV, respectively. These results indicate that the H_2SO_4-NH_3 reaction is not favored for the generation of NH_4HSO_4 in the standard SCR atmosphere. Figures 1 (c) and (d) show another route to form NH_4HSO_4 directly via the reaction of SO_3 with H_2O and NH_3, calculated using cluster and periodical models. The results show that the energy barrier of this tri-molecule reaction is only 0.1 eV (periodical boundary) and 0.47 eV (cluster), which is significantly lower than that of the bi-molecule H_2SO_4-NH_3 reaction. According to the previous studies of the aerosol particles nucleation [56, 57], H_2O molecules could act as proton transporters and actively participate in the reactions between ammonia and sulfur oxides. Thus, the NH_3-H_2O-SO_2 reaction has almost no barrier and is the most favorable route for NH_4HSO_4 formation in

low-temperature NH_3-SCR processes.

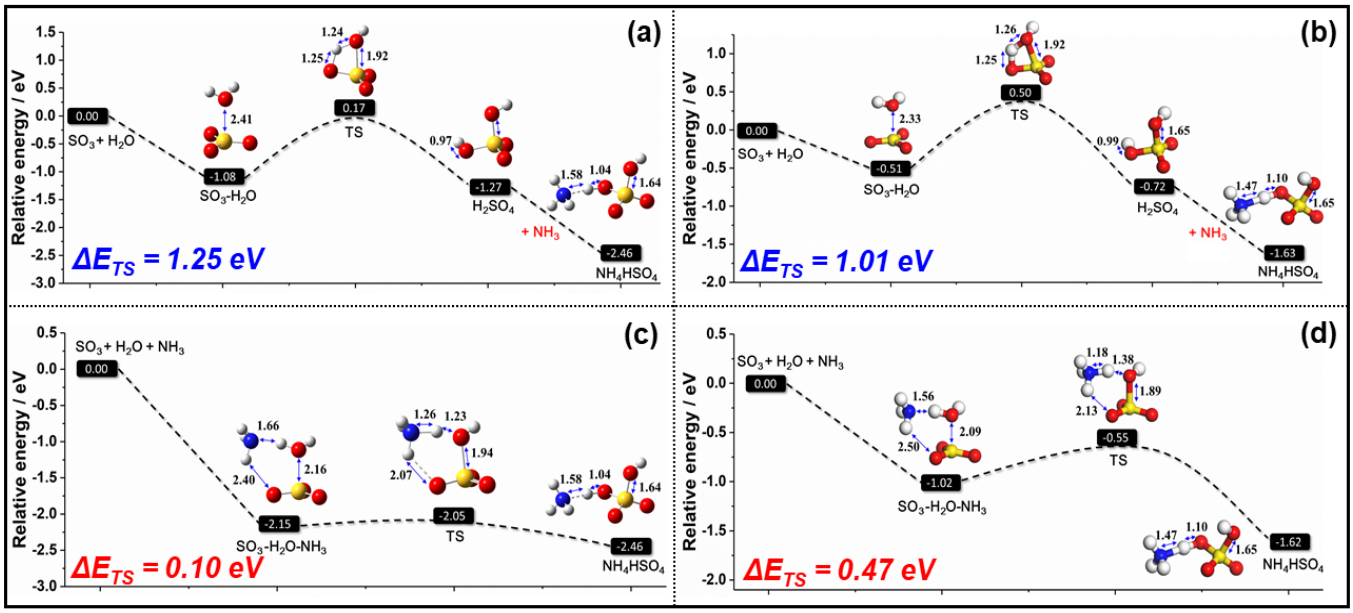

Figure 1. Structure and energy profiles of the different NH_4HSO_4 formation routes. Two series of calculations: (a, c) cluster-based calculations; (b, d) periodical calculations. Oxygen is red, nitrogen is blue, hydrogen is white, and sulfur is yellow.

Since NH_4HSO_4 can be easily formed in the gas phase in flue gas, in the following study, the NH_4HSO_4 poisoning catalyst model was simulated using a whole NH_4HSO_4 molecule directly adsorbed on the surface of the catalyst. The calculated adsorption energies of NH_4HSO_4 on the Ti and VTi catalyst were -1.74 eV and -1.13 eV, respectively, indicating that the adsorption of NH_4HSO_4 on the surface of both catalysts is extremely favorable. As shown in Figure 2 (c) and (f), the SO_4^{2-} of NH_4HSO_4 is tightly bound to the Ti-O-Ti site of the Ti and VTi catalysts. In the Ti-p structure, a close chemical bond with the length of 1.57 Å formed between the S atom and the surface O atoms. For the VTi-p structure, a similar S-O-Ti bond with the length of 1.59 Å was formed, and additionally, we also found a weak H-O bond between the H atom of NH_4^+ and the O atom of the V-O-Ti site.

The FTIR, SEM and BET characterizations were used to verify the deposited NH_4HSO_4 model presented in Figure 2 (c, f). As shown in Figure 2 (g), the FTIR spectra of NH_4HSO_4-deposited samples shows peaks at 1400 cm^{-1}, 1210 (1206) cm^{-1}, 1139 (1137) cm^{-1} and 1054 cm^{-1}. The peak at 1400 cm^{-1} can be assigned to the symmetric bending vibration of the N-H in NH_4^+, while the peaks at 1210 (1206) cm^{-1} and 1139 (1137) cm^{-1} can be ascribed to the asymmetrical and symmetrical stretching vibrations of S=O from SO_4^{2-} [33, 34]. At 1054 cm^{-1}, this peak is associated with the asymmetrical stretching of the S-O-Ti vibrations [58].

Moreover, the fresh Ti and VTi samples had higher BET specific surface areas of 47.1 and 48.1 m^2/g, respectively, while the specific surface area of both catalysts dropped to 24.4 and 25.7 m^2/g, respectively when NH_4HSO_4 was deposited onto the catalyst surfaces. However, no sizeable NH_4HSO_4 particles were observed on the surface of the processed catalyst, as shown in the SEM images (Figure 2 (h, i, j, k)). This suggests that the NH_4HSO_4 was well-distributed on the catalyst surfaces and covered the catalyst particles, which agrees with our previous work [34]. Isolated particles of the catalyst were also found to agglomerate to form larger particles due to the adhesive NH_4HSO_4, resulting in the decreased surface area.

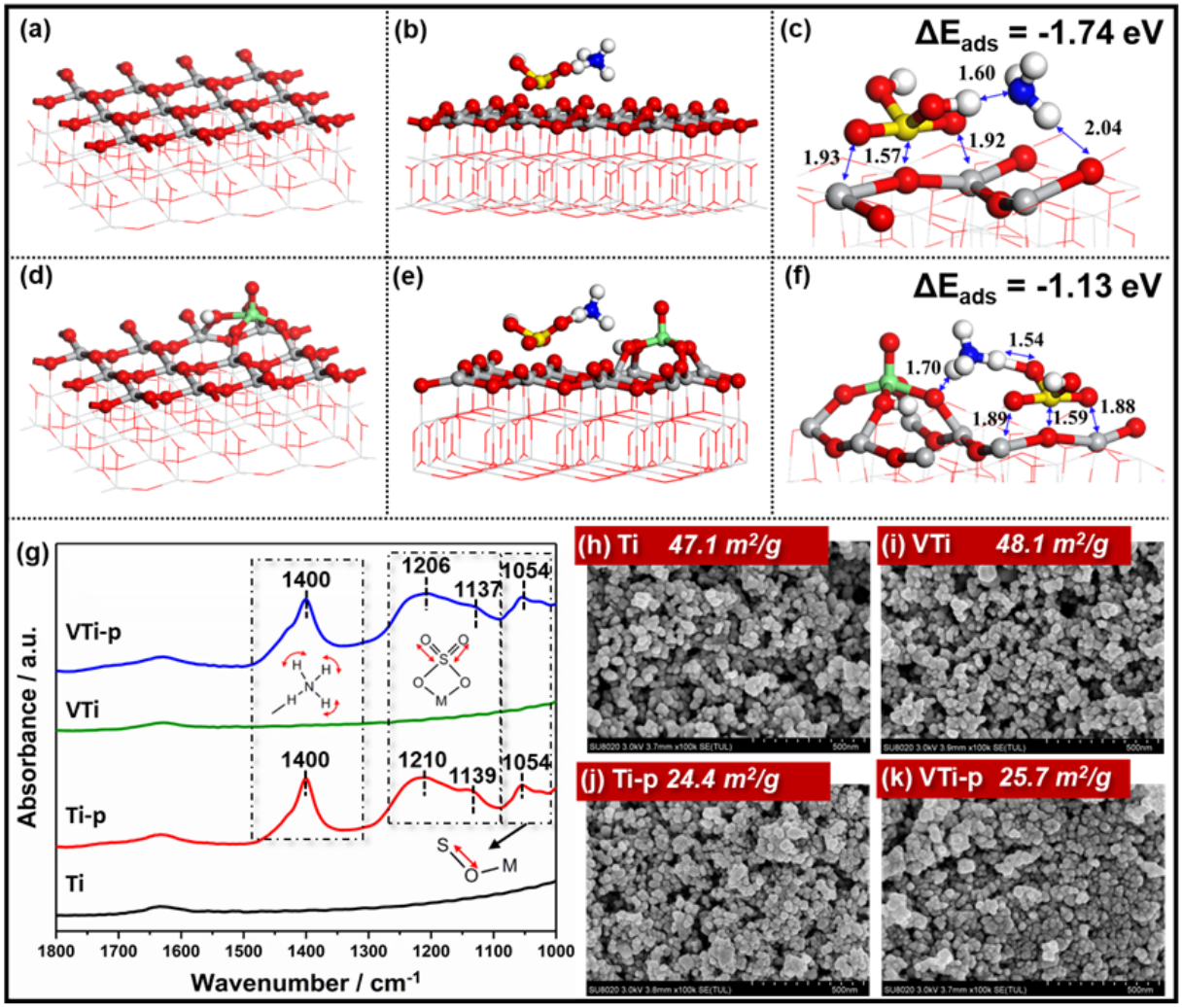

Figure 2. Theoretical stationary structures of (a) TiO_2; (b, c) NH_4HSO_4 deposited on TiO_2 (Ti-p); (d) V_2O_5-TiO_2; (e, f) NH_4HSO_4 deposited on V_2O_5-TiO_2 (VTi-p); Oxygen - red, titania - gray, vanadium - green, nitrogen - blue, hydrogen – white, and sulfur - yellow.

(g) Experimental FTIR spectra of the Ti, Ti-p, VTi and VTi-p catalysts;

SEM images and BET surface area of the (h) TiO_2, (i) VTi, (j) Ti-p, (k) VTi-p catalyst.

3.2 The reaction behavior of NH_4HSO_4 in different atmospheres

3.2.1 Experimental reaction profiles

The in-situ DRIFTS experiment was carried out to help understand the reactivity of the NH_4^+ in NH_4HSO_4 over the catalyst surface under standard SCR conditions. Free NH_3 adsorbed onto

the fresh VTi catalyst was used as a reference. As shown in Figure 3 (a), two bands at 1423 and 1221 cm^{-1} appeared after introducing NH_3 onto the VTi catalyst. These two bands can be assigned to the NH_4^+ at the Bronsted acid site and NH_3^* at the Lewis acid site, respectively. After NH_3 pretreatment for 25 mins, the NH_3 feed was switched off, and a mixture of NO and O_2 was fed into the reactor. When using the NO/O_2 mixture, the intensity of the bands related to NH_3 species decreased gradually over time. The peaks at 1423 and 1221 cm^{-1} had almost disappeared at 25 mins, which indicates that the absorbed NH_3 can react effectively with NO over the VTi catalyst at 250 ^oC (Eley-Rideal mechanism). Figure 3 (b) presents the in-situ DRIFT spectra of the VTi-p catalyst whilst it was being exposed to a mixture of NO and O_2. In this process, the intensities of NH_4^+ (1432 cm^{-1}) and sulfate species (1247 cm^{-1}, 1135 cm^{-1}, and 1049 cm^{-1}) were almost unchanged. These bands can still be observed even at 212 mins. These findings suggest that NH_4^+ from NH_4HSO_4 is noticeably less active than the adsorbed ammonium species on the catalyst surface in NO/O_2. The result indicates that the decomposition of the deposited NH_4HSO_4 via the reaction with NO was slow at 250 ^oC, and thus NH_4HSO_4 would continuously deposit on the catalyst surface in low-temperature SCR processes.

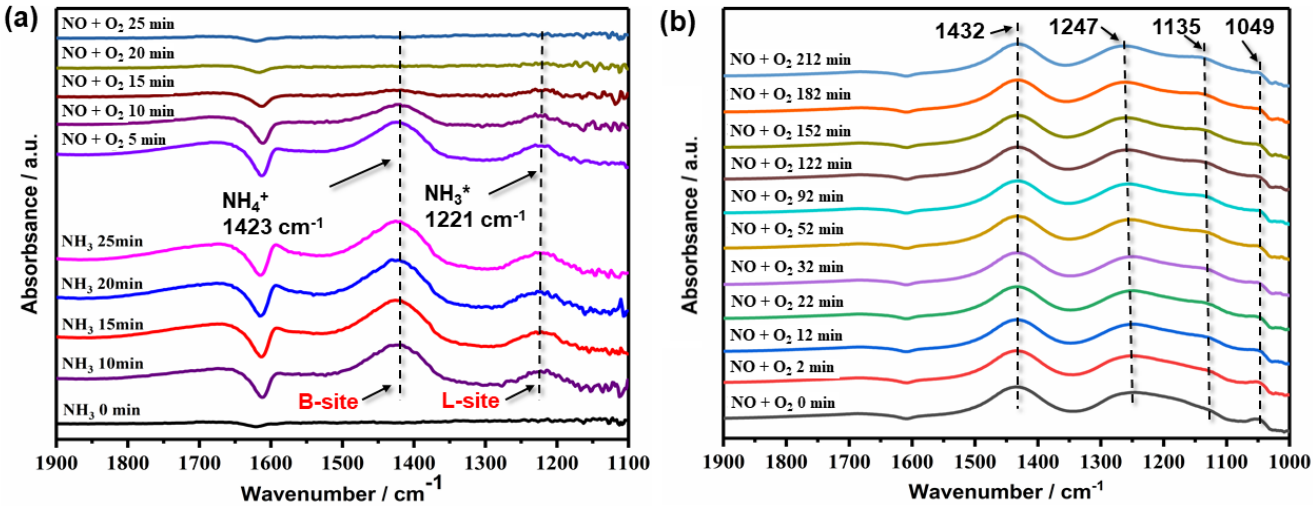

Figure 3. (a) In-situ DRIFT spectra of the VTi catalyst pretreated by NH_3 for 25 mins and then exposed to NO + O_2 for 25 mins; (b) In-situ DRIFT spectra of the VTi-p catalyst in a flow of NO + O_2 for 212 mins.

In this study, temperature-programed decomposition of NH_4HSO_4 on the catalyst surface was also investigated in a more oxidative atmosphere ($NO/NO_2/O_2$). Figure 4 shows that it is difficult to decompose the NH_4HSO_4 formed on the catalyst surface in an NO/O_2 mixture at low temperatures. The reaction between NH_4HSO_4 and the NO/O_2 mixture was only observed above 300 ^oC. The standard NH_3-SCR reaction over the Ti and VTi catalysts was also carried out for comparison. As shown in the inserted figure in Figure 4, the reaction between NH_4HSO_4 and NO is more intense than the NH_3-SCR reaction over the Ti catalyst. For example, the conversion of NO_x reached 36% in the reaction between NH_4HSO_4 and NO over the Ti catalyst at 400 ^oC, while the conversion of NO_x in the reaction between NO and NH_3 was only 22% at the same reaction temperature. By contrast, the NO_x conversion during the reaction between NH_3 and NO was much higher than that of the reaction between NH_4HSO_4 and NO at the temperature range of 200 - 450 ^oC over the VTi catalyst. For the Ti catalyst, the deposition of

NH_4HSO_4 produced the $TiSO_4$ acid site, which exhibited higher SCR reactivity compared to the fresh TiO_2 surface without NH_4HSO_4 deposition [58-61]. However, for the VTi catalyst, the active sites and the mechanism of the reaction between NH_4HSO_4 and NO are still unknown.

Moreover, adding NO_2 enhanced the reaction of NH_4HSO_4 with NO_x on the VTi catalyst. However, this promotion effect of NO_2 was not observed on the Ti catalyst, which indicates that the $NO/NO_2/O_2$ mixture can only effectively react with NH_4HSO_4 on the vanadia-loaded TiO_2 catalyst. Thus, it is important to understand the role of vanadium active sites in the reaction of NH_4HSO_4 with NO_x. In the next section, DFT calculations will be implemented to gain deeper insights into the reaction of NH_4HSO_4 with NO_x on the VTi catalyst.

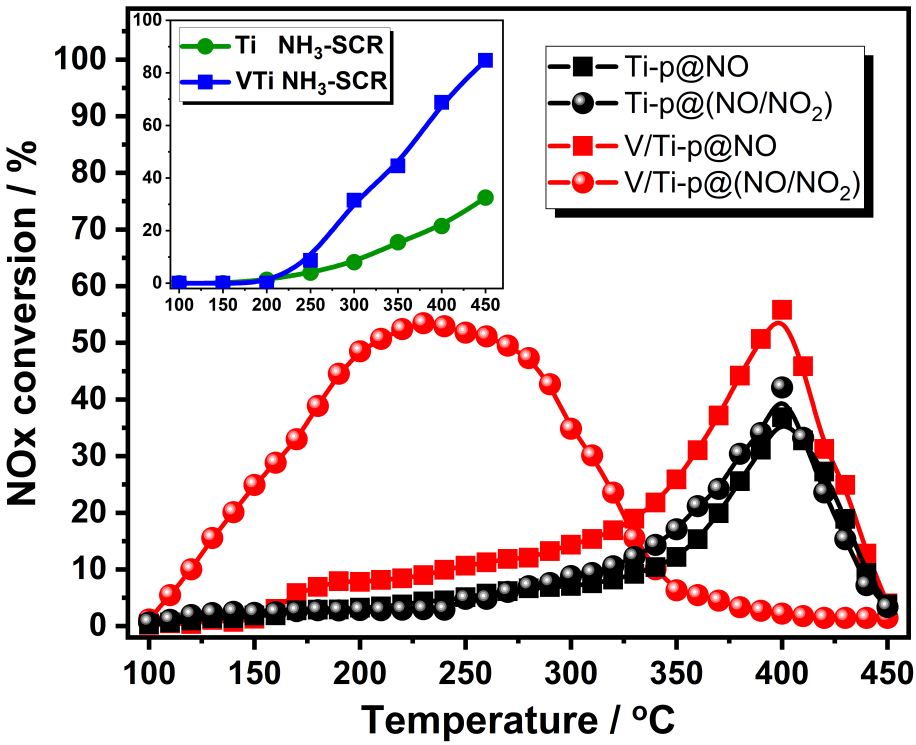

Figure 4. The TPSR of deposited NH_4HSO_4 with different gas mixtures over VTi and Ti catalysts and the NH_3-SCR performance of VTi and Ti catalysts (inserted).

3.2.2 Theoretical pathways of the NH_4HSO_4 reaction on the VTi catalyst

We first calculated the commonly accepted mechanism of the NH_3-SCR reaction on the VTi catalyst and then calculated the reaction mechanism of NH_4HSO_4 with NO. Figure 5 shows that NH_3 can be effectively adsorbed onto the V-OH Bronsted acid sites of the V-Ti catalyst. The adsorption of NH_3 (Figure 5(a)) is an exothermic reaction with an activation energy of 0.94 eV. According to the E-R reaction mechanism [62], the adsorbed NH_3 reacts with the gas phase NO to form H_2NNO (Figure 5(b) to (d)), which can rapidly decompose to N_2 and H_2O. The formation of H_2NNO (Figure 5(c)) is the rate-determining-step in the NH_3-SCR reaction, which corresponds to an activation energy (ΔE_{TS}) of 0.73 eV (from -1.10 eV to -0.37 eV). The reduced VO_3H_2 site with the V^{4+} ion contains two hydroxylated V-OH sites (Figure 5(e)). In the reaction of NO with the deposited NH_4HSO_4, the reaction route was similar to that in the NH_3-SCR reaction. An NO molecule approached the NH_4^+ of NH_4HSO_4 around the V^{5+} site (Figure 5b'), leading to the formation of a H_2NNO intermediate through the bonding of the two N atoms and the reduction of the adjacent V^{5+} site (Figure 5d') simultaneously. The activation energy for the formation of H_2NNO in the reaction between NH_4HSO_4 and NO was 0.93 eV (from -1.33 eV to -0.96 eV), which is higher than that in the standard NH_3-SCR reaction (0.73 eV). The higher energy barrier indicates that the reaction between NH_4HSO_4 and NO was slower than that between free NH_3 (adsorbed on VTi catalyst) and NO, which is consistent with the experimental results. Finally, the sulfate species of NH_4HSO_4 remained on the catalyst surface after NH_4^+ was consumed by NO (Figure 5e').

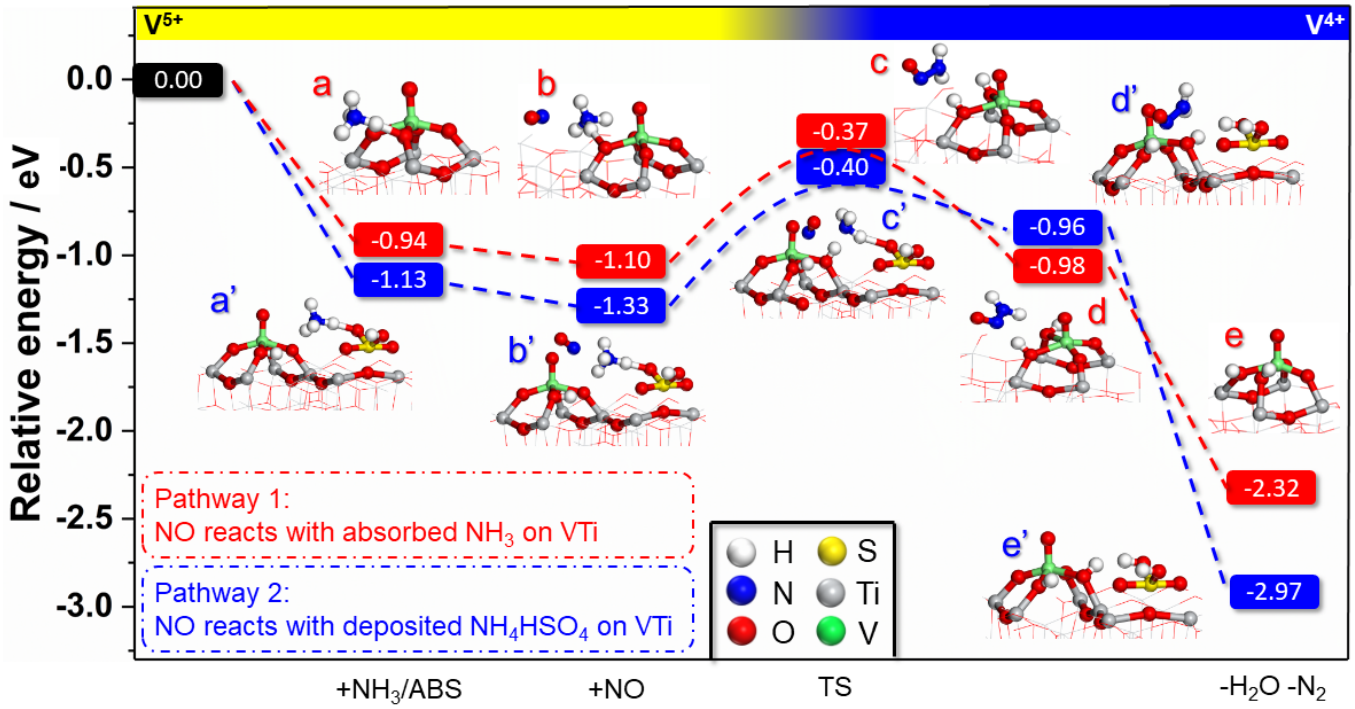

Figure 5. Theoretical energy and structure profiles for the reaction of NO with deposited NH_4HSO_4 and absorbed NH_3 over the VTi catalyst.

3.3 The promotion mechanism of NO_2 on the reaction of NH_4HSO_4

The reaction of NH_4HSO_4 with NO over the VTi catalyst is a redox process. The V^{5+} ion was reduced to V^{4+} after the formation of H_2NNO in the reaction of NH_4HSO_4 and NO. The reoxidation of V^{4+} to V^{5+} is a crucial step in completing the catalytic cycle. In the NH_3-SCR processes, it is well known that NO_2 is a better oxidizing agent compared to O_2 and can efficiently contribute to the reoxidation process in the NH_3-SCR cycle [52, 63]. As shown in Figure S1, the results of the TPSR reaction from 100 to 400 ^oC indicate that a sole NO_2 rarely reacts with the NH_4^+ of the deposited NH_4HSO_4. In the rapid reaction between NH_4HSO_4 and an NO/NO_2 mixture, the consumption of NO and NO_2 was almost the same, as shown in Figure S2. This finding is consistent with the optimal NO/NO_2 ratio of 1:1 in the 'Fast SCR' reaction.

It is possible that NO_2 also participated in the reoxidation in the reaction between NH_4HSO_4 and NO_x. In the next section, XPS characterization and TRM experiments were presented to investigate this promotion effect over the VTi catalyst. Additionally, theoretical calculations were also performed to understand the mechanism on the atomic level.

3.3.1 XPS analysis

In the XPS characterization, the VTi-p catalyst samples were pretreated in either an NO/O_2 atmosphere (500 ppm NO, 5% O_2 and N_2 as balance) or an $NO/NO_2/O_2$ atmosphere (250 ppm NO, 250 ppm NO_2, 5% O_2 and N_2 as balance) at 250 ^oC for 1 hour, respectively. The samples were denoted as VTi-p@NO and VTi-p@(NO/NO_2). Figure 6 shows the XPS analysis of the catalysts after pretreatment using different gas compositions in order to understand the variation in the chemical status of the catalytic surface before and after treatment.

Figure 6(a) shows the overlapping V 2p signals of the samples. The XPS spectra can be deconvoluted into two peaks assigned to the V^{5+} and V^{4+} species. The ratio, $V^{5+}/(V^{5+}+V^{4+})$, was determined through the calculation of the integrated peak area of V^{5+} and V^{4+} species. Introducing NH_4HSO_4 to the VTi catalyst had a limited effect on the surface ratio $V^{5+}/(V^{5+}+V^{4+})$ of the VTi catalyst, which suggests little interaction between NH_4HSO_4 and V sites. After processing in the NO/O_2 mixture, the $V^{5+}/(V^{5+}+V^{4+})$ ratio significantly decreased to 58%, which means O_2 cannot effectively reoxidize the reduced V^{4+} in this reaction at 250 ^oC. By contrast, the ratio $V^{5+}/(V^{5+}+V^{4+})$ was maintained at 71% after processing in the $NO/NO_2/O_2$ atmosphere. This result reveals that NO_2 can oxidize the reduced catalyst more effectively than O_2 in the reaction of deposited NH_4HSO_4 with NO_x.

The O 1s spectra show the formation of the chemically adsorbed oxygen (O_α) and lattice oxygen (O_β) (Figure 6(b)). Compared to the catalyst without deposition, the ratio $O_\alpha/(O_\alpha+O_\beta)$ increased when NH_4HSO_4 was deposited on the catalyst surface. This finding is due to the loading of oxygen-containing sulfate on the catalyst surfaces resulting in the generation of more surface adsorbed oxygen. After processing in the NO/O_2 and $NO/NO_2/O_2$ atmospheres, the ratio $O_\alpha/(O_\alpha+O_\beta)$ of the samples was almost the same, which indicates the sulfate species might remain on the catalyst surfaces. The S 1s spectra shown in Figure 6(c) further proved that it is difficult for S containing species to escape from the catalyst surface. The Ti 2p photoelectron peaks (Figure 6(d)) shifted towards higher binding energies after the deposition of NH_4HSO_4 on the catalyst surface as the electrons around Ti atoms deviate towards the S=O sites of the sulfate species. A greater shift of the binding energy of the Ti 2p photoelectron peaks can be found for the samples treated in the $NO/NO_2/O_2$ atmosphere. This phenomenon reveals that the S=O from the acidic sulfate sites can strongly attract electrons from the surface Ti species and the consumption of NH_4^+ from NH_4HSO_4 can enhance the interaction between the sulfate species and the catalyst surface.

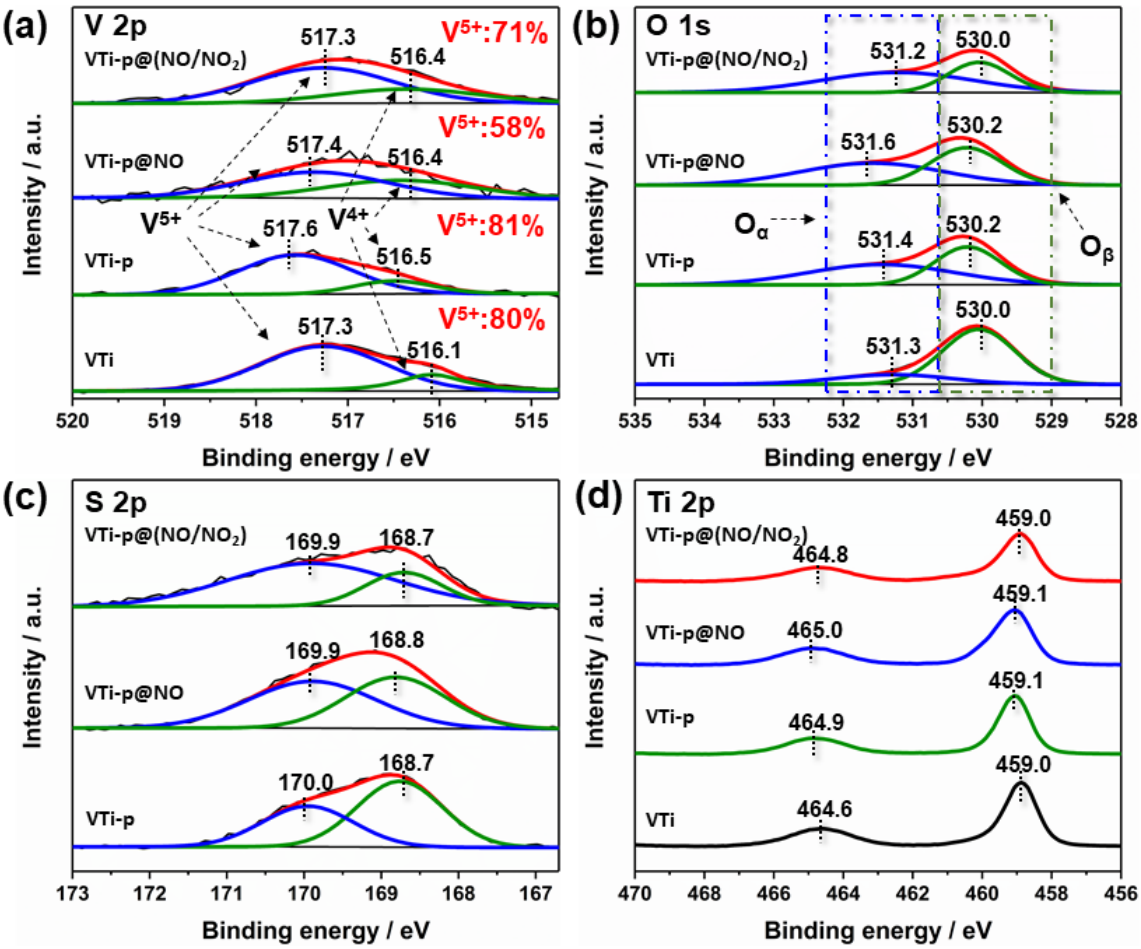

Figure 6. XPS spectra of the samples (a) V 2p; (b) O 1s; (c) S 2p; (d) Ti 2p.

3.3.2 TRM experiment

To further probe the reoxidation effect of O_2 and NO_2, the TRM experiment was carried out. The VTi-p sample was treated repeatedly in reducing and oxidizing atmospheres. Figure 7 shows the details of the reactions. In these reactions, the concentrations of NO and NO_2 were recorded to analyze the consumption of the respective components. We did not provide the concentration of O_2 since it did not noticeably change during these reactions. The reaction in the absence of a catalyst was performed for comparison. These black curves were regarded as the background to calculate the changes of NO and NO_2. The difference between the detected data and the background means the concentration of NO/NO_2 consumed in the reactions.

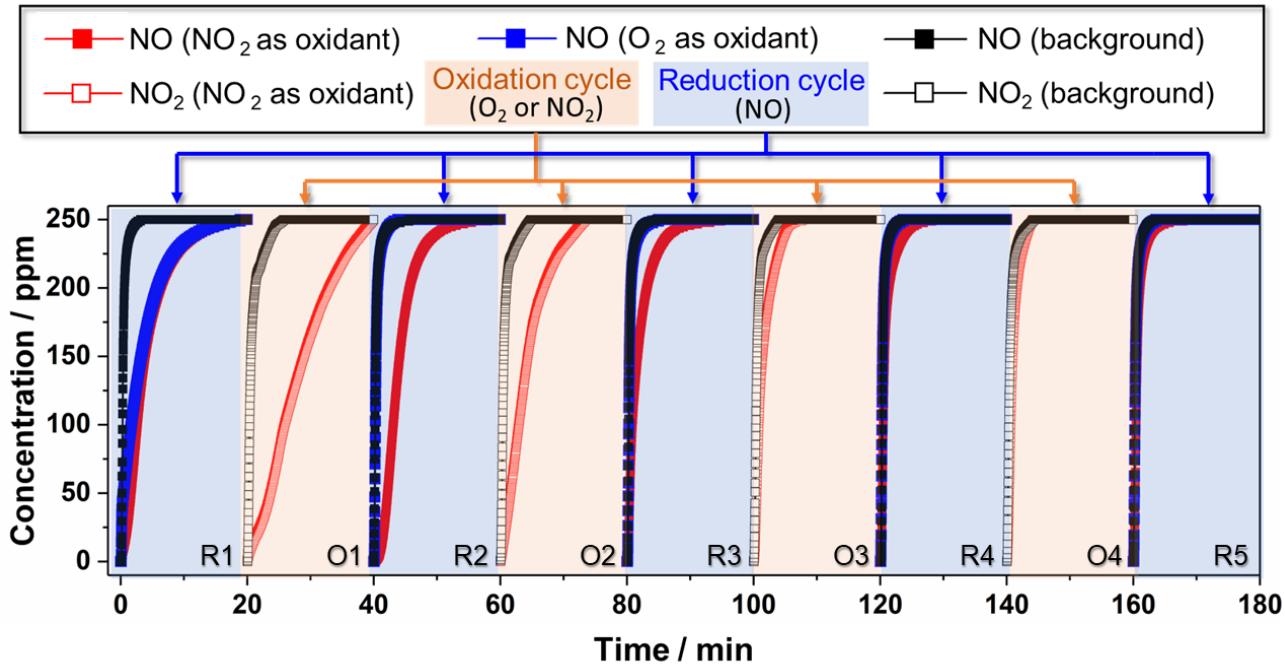

Figure 7. TRM experiments for the reaction of NH_4HSO_4 on the VTi-p catalyst with different oxidizing agents (Reduction cycle: the VTi-p sample was treated in 250 ppm NO; reoxidation cycle: the catalyst was treated in 5 vol.% O_2 or 250 ppm NO_2; black solid square: the concentration of NO as the background in the reducing cycle; black empty square: the concentration of NO_2 as the background in the reoxidation cycle; red solid square: the concentration of NO in reduction cycle when NO_2 was used as the reoxidizing agent; red empty square: the concentration of NO_2 in the reoxidation cycle when NO_2 was used as the reoxidizing agent; blue solid square: the concentration of NO in the reduction cycle when O_2 was used as the reoxidizing agent)

Using NO_2 as an oxidant, as shown in the R1 (meaning first reduction step) region of Figure 7, 250 ppm NO was fed into the reactor containing the VTi-p catalyst. During this stage, the VTi-p catalyst was reduced due to the reaction of NH_4HSO_4 with NO until NO reached its maximum concentration (at T = 20 min), which confirms the completion of the reduction of all

the reactive V^{5+} species in the catalyst to V^{4+}. The NO feed was then switched off, 250 ppm NO_2 as the oxidant was fed to the reactor. As shown in the O1 (meaning first oxidation step) region, the outlet NO_2 concentration increased slowly and reached 250 ppm at 20 min. The significant reduction of NO_2 indicates that the oxidation of the reduced VTi-p catalyst by NO_2 occurs during this stage. In the next cycle, the NO_2 feed was replaced by the NO feed. The consumption of the NO occurred again in the R2 region, which indicates the reduced V^{4+} sites were effectively oxidized to V^{5+} by NO_2 and then continue to participate in the reaction with NH_4HSO_4. The reduction-reoxidation cycle proceeded until the NH_4HSO_4 on the catalyst surface was completely consumed by NO. As shown in the O4 and R5 region (oxidation-reduction), almost no NO and NO_2 were consumed, suggesting that NH_4HSO_4 reaction on the catalyst surface had completed since no redox reaction proceeded on the catalytic surface.

Using O_2 as an oxidant, the NO consumption was only found in the first reduction cycle (shown in Figure 7 R1 region). In the second and successive reduction cycles, no noticeable NO consumption was observed. Although the concentration of O_2 was not given since its change was neglectable, the NO consumption profiles in the reduction cycles indicated that O_2 was unable to reoxidize the reduced catalyst at 250 ^oC. Consequently, the deposited NH_4HSO_4 on the V-Ti catalyst cannot be continuously consumed in the NO/O_2 atmosphere since O_2 cannot effectively reoxidize the reduced catalyst.

The results of the TRM experiments reveal that the reactive V^{5+} sites could be easily reduced in the reaction of NH_4HSO_4 with NO. However, the reoxidation process differed when using O_2 and NO_2 as the oxidant. We can thus hypothesize the reoxidation of V^{4+} is the rate-determining step in the reaction of deposited NH_4HSO_4 with NO, while NO_2 is a better

oxidizing agent compared to O_2, which has also been demonstrated by the results of XPS characterization in section 3.3.1.

3.3.3 The theoretical mechanism of V^{4+} reoxidation by different oxidants

Figure 8 shows the energy diagram and structures for the reoxidation reaction over the reduced VTi-p catalyst using O_2 or NO_2 as the oxidant. The structure (V^{4+}) generated after the interaction of the VTi-p catalyst with NO was regarded as the initial reduced structure for the reoxidation step. In the NH_3-SCR reaction over a fresh V_2O_5/TiO_2 catalyst, Arnarson et al. [52] proposed an O_2 reoxidation route where a H_2O molecule formed and desorbed from the VO_3H_2 structure, leaving VO_3H_2 in a more distorted geometry and more prone towards the reaction with O_2. This pathway was also applied to analyze the reoxidation of the VTi-p catalyst by O_2. As shown in Figure 8(b)(a-d), H_2O is formed via the reaction between two V-OH-Ti sites which is followed by the generation of a distorted V-O-Ti_2 site. The activation energy of H_2O formation was ΔE_{ab} = 0.27 eV. The formed H_2O desorbed from the catalyst surface (Figure 8(b)d) with an endothermic energy of 1.38 eV. The reaction of O_2 with the distorted V-O-Ti is strongly exothermic (-2.27 eV), which suggests that the V-O-Ti intermediate can be easily oxidized by O_2 to form a Ti-O-V-(O_2*)-Ti^- (V^{5+}) structure (Figure 8(b)e). Subsequently, NO can actively participate in this reaction since NO has an unpaired electron in its highest molecular orbital. As shown in Figure 8(a), it is energetically favorable (ΔE_{ef} = -1.12 eV), that NO molecule was absorbed on the V-(O_2*)-Ti structure to form a V-(O_2NO)-Ti intermediate. The break of the internal O_2^{2-} bond has an energy barrier of 1.51 eV and the generation of a V-(NO_3)-Ti structure is exothermic by -1.36 eV. Finally, the NO_2 desorbed to the gas phase by

consuming energy (1.16 eV), and the reoxidized structure formed. Combining with the energy profile of the reduction process (with an energy barrier of 0.93 eV), the higher energy barrier (1.51 eV) in the reoxidation process indicates that the reoxidation of V^{4+} to V^{5+} is the rate-determining step for the reaction between NO/O_2 and NH_4HSO_4 over the VTi catalyst.

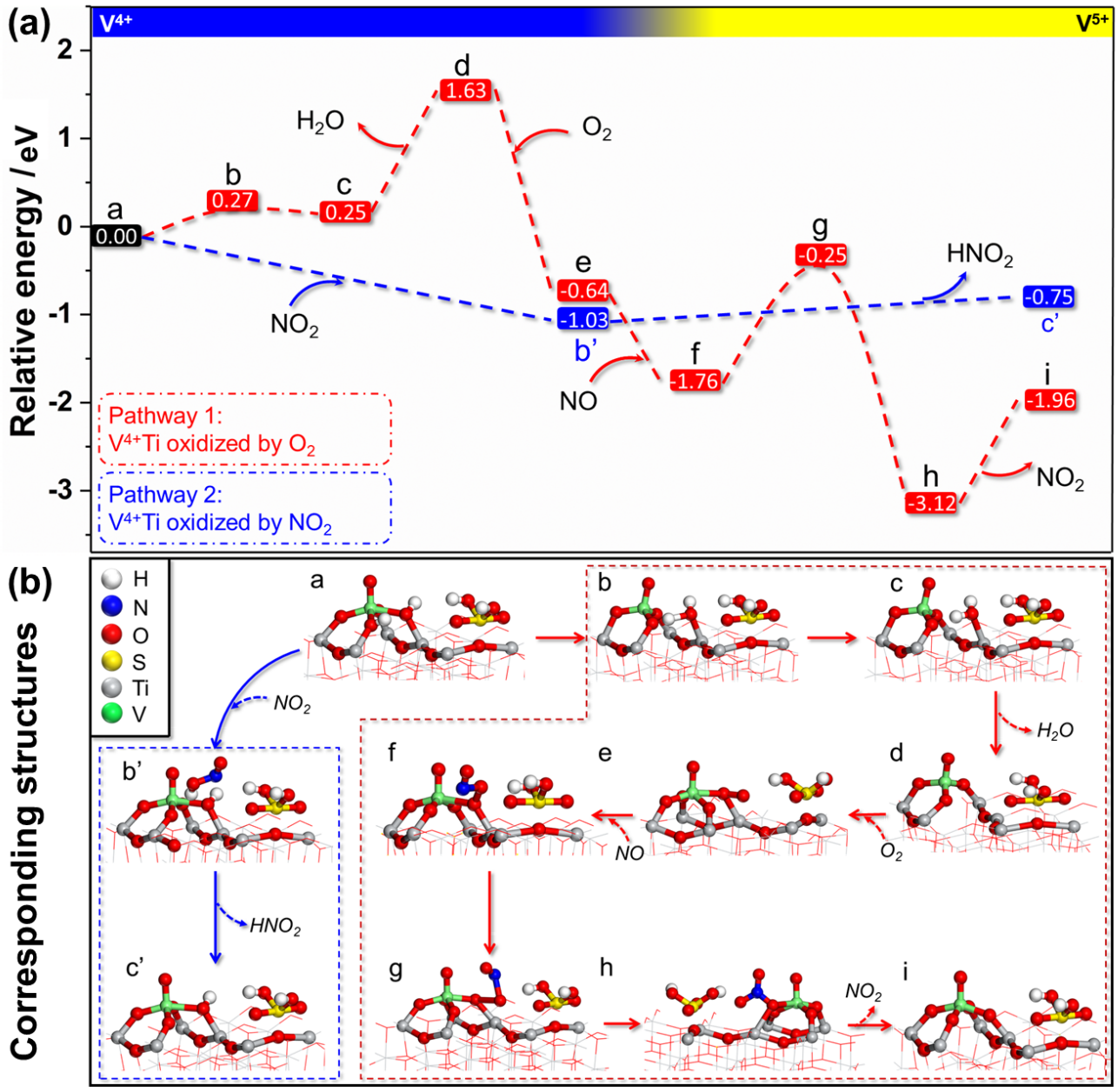

Figure 8. Energy diagrams and stationary structures for the reoxidation reaction of the reduced VTi-p catalyst (O_2 or NO_2 as the oxidant).

Previous studies revealed that NO_2 is a better oxidant than O_2 for the reoxidation of the active sites in SCR reactions [63, 64]. In this study, NO_2 also exhibited an excellent ability to oxidize the reduced V/Ti-p catalyst. As shown in Figure 8(b)(a-b'), NO_2 can easily capture a H atom from the reduced V-OH-Ti site when it approaches the catalyst surface. HNO_2* is produced releasing energy (1.03 eV) and no transition state could be found for this process, which corresponds with results from previous research [52]. After this reaction, the reduced V^{4+} was reoxidized to V^{5+} (Figure 8(b)b') and both the structure and electronic properties of the VTi catalyst were effectively restored. The desorption of HNO_2 from the VO_3H site is endothermic by 0.28 eV (from -1.03 eV to -0.75 eV). The energy profile indicates that the reoxidation of V^{4+} by NO_2 has no barrier. Consequently, the formation of NH_2NO in the reduction process is the rate-determining step in the reaction between NO/NO_2 and NH_4HSO_4 on the VTi catalyst, which is different to that of the reaction between NO/O_2 and NH_4HSO_4.

3.3.4 The reaction of NH_4HSO_4 with HNO_2 on the VTi catalyst

The formed HNO_2 can also react with the NH_4HSO_4 deposited on the catalyst surface, as presented in Figure 9. Firstly, the O atom of HNO_2 can weakly bond with a H atom of NH_4HSO_4 with an exothermic energy of -0.25 eV. The products of the reaction between HNO_2 and the ammonia species in NH_4HSO_4 were H_2O and H_2NNO, which is similar to that reported in the fast SCR reactions [65, 66]. The energy barrier of the reaction between HNO_2 and the ammonia species is 1.15 eV. The H_2O molecule desorbed after absorbing the energy (0.2 eV), and the H_2NNO molecule transformed to N_2 and H_2O with an exothermic energy of 1.87 eV. Although

the reaction between NH_4HSO_4 and HNO_2 takes place around the V site, there is no electron transfer between the reactant and V site. After the reaction of HNO_2 with the deposited NH_4HSO_4 on the VTi catalyst surface, the structure and electronic properties of the V^{5+} (VO_3H) site remained unchanged.

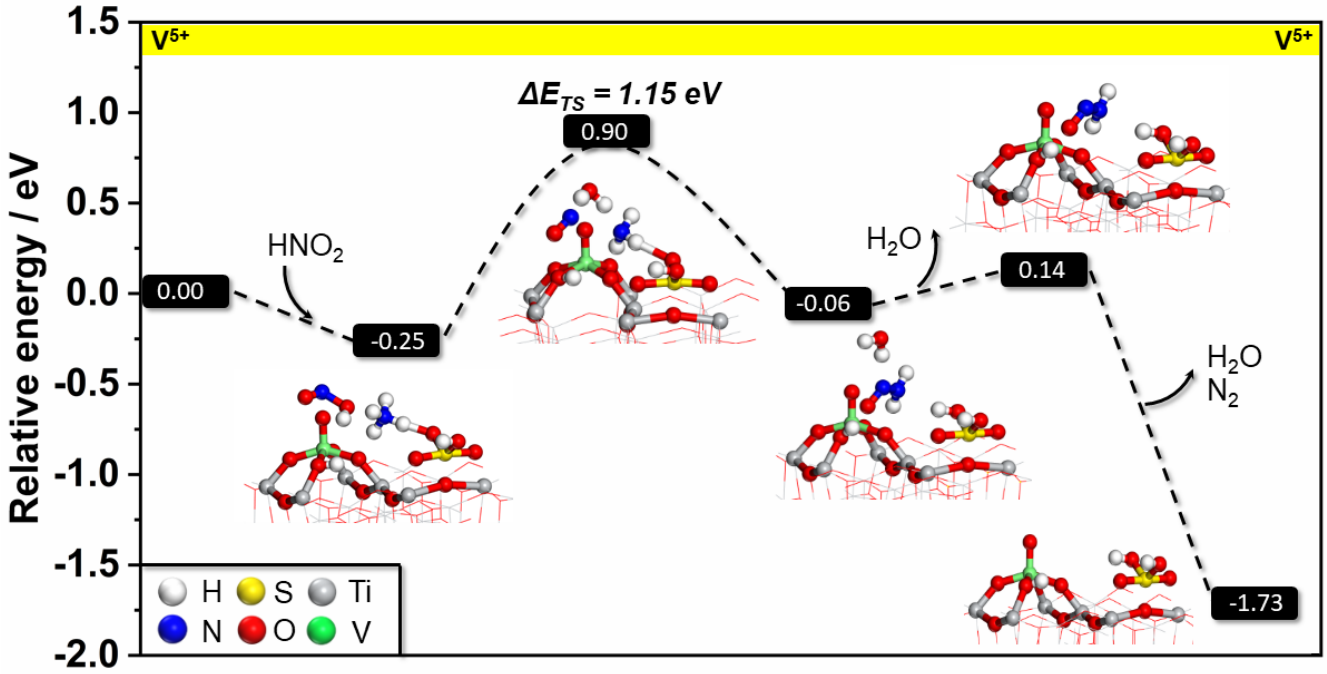

Figure 9. Energy and structure profiles for the reaction between HNO_2 and deposited NH_4HSO_4 over the VTi catalyst.

3.4 Discussion

VWTi is a successful commercial SCR catalyst with a strong resistance to sulfur poisoning. As shown in Figure 10(a), the sulfated VWTi catalyst (VWTi-S) exhibits almost the same activity as the fresh VWTi catalyst in both standard and fast SCR reactions. In addition, VWTi-S shows a better N_2 selectivity than that of VWTi at high temperatures (>400 ^oC) since sulfation reduces the oxidation of NH_3 on the catalyst. However, this does not mean that the commercial VWTi catalyst can maintain its deNOx activity in an industrial flue gas containing SO_2 and

H_2O. The deposition of NH_4HSO_4 can inevitably deactivate the VWTi catalyst. As shown in Figure 11, the SCR activity of the VWTi catalyst decreased continuously in the presence of H_2O and SO_2 at 250 ^oC. In contrast, the VWTi catalyst exhibited an excellent sulfur tolerance when NO_2 was added to the reaction. The fast SCR activity of the VWTi catalyst can be well maintained after 10 hours in the presence of H_2O and SO_2 at 250 ^oC. Moreover, the concentration of N_2O was also monitored during these tests (shown in Figure S4). The results show that the N_2 selectivity can be maintained above 98% during the test.

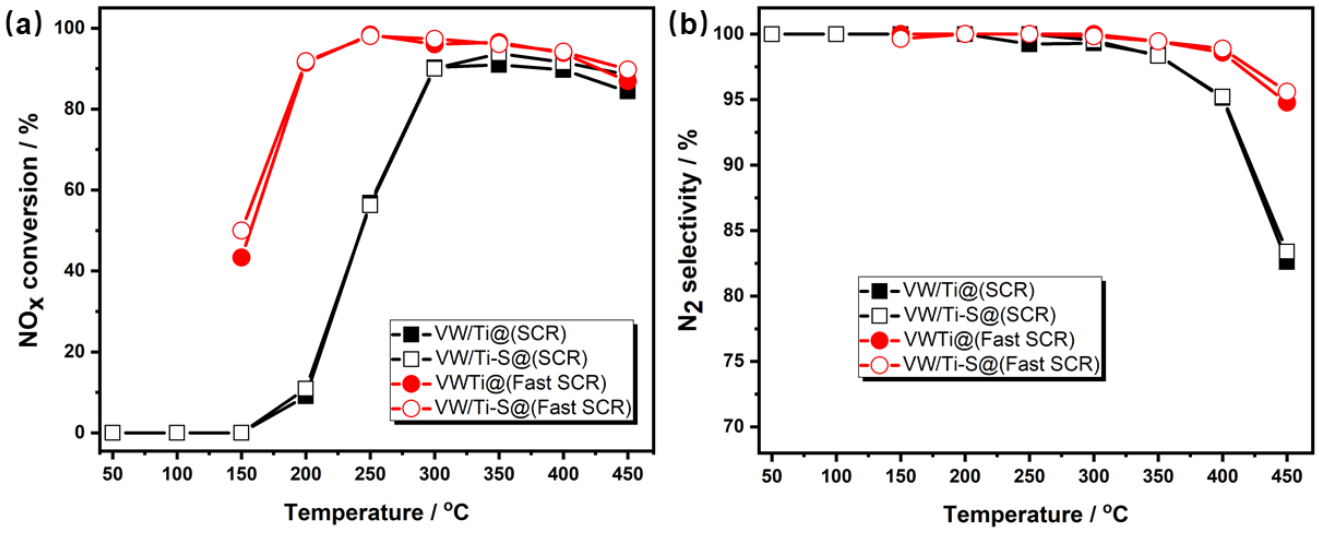

Figure 10. (a) NO_x conversion; (b) N_2 selectivity of the standard and fast SCR reactions on the VWTi and VWTi-S catalysts.

The rate difference between the deposition and decomposition of NH_4HSO_4 on the catalyst surface plays a significant role in determining the long-term stability of the low-temperature SCR operated in SO_2-containing flue gas. Our results have demonstrated that the sulfur resistance of the commercial VWTi catalyst can be significantly enhanced by rapidly decomposing NH_4HSO_4 on the catalytic surface using an NO/NO_2 mixture. Therefore,

optimizing the reaction atmosphere opens a route other than the strategical catalyst design & optimization to tackle the challenge of sulfur poisoning in the low-temperature SCR processes.

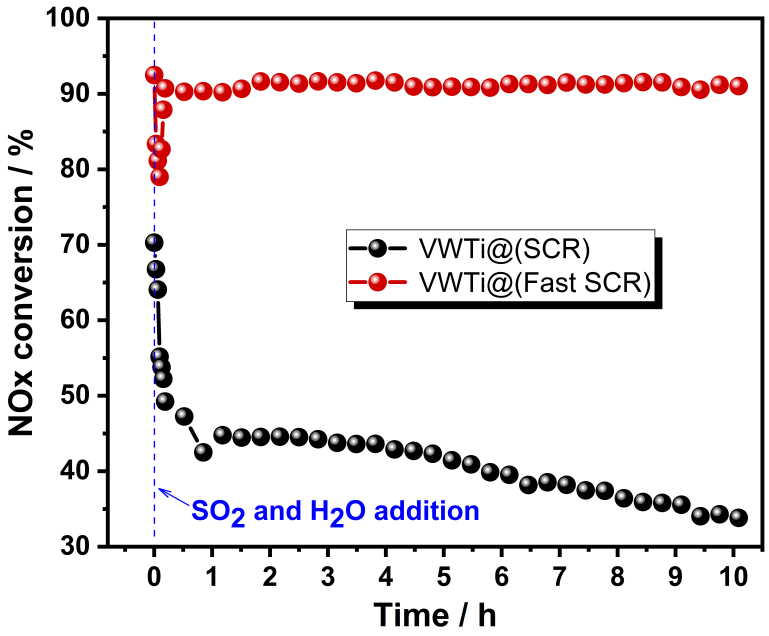

Figure 11. Sulfur tolerance test of the commercial VWTi catalyst in the standard and fast SCR reactions.

4. Conclusions

In this study, the deposition and decomposition of NH_4HSO_4 on the VTi catalyst have been investigated by DFT modeling coupled with catalyst characterization techniques. A nearly barrierless route for the formation NH_4HSO_4 in the gas phase was proposed and the structure of the deposited NH_4HSO_4 on the VTi catalyst was presented. More importantly, the complete mechanisms in the reactions of NH_4HSO_4 with NO_x (NO/O_2 or $NO/NO_2/O_2$ mixtures) on the catalyst have been proposed and discussed. In addition, sulfur tolerance testing for the VWTi catalyst has been carried out to understand the decomposition of NH_4HSO_4 over the catalyst surface and consider the long-term stability of the low-temperature SCR processes. The major

findings of this work can be summarized as follows.

1. NH_4HSO_4 can be easily formed in the gas phase through the nucleation of NH_3, H_2O, and SO_3 in NH_3-SCR processes. The deposition of NH_4HSO_4 on the VTi catalyst is extremely favorable with a tight Ti-O-S bond.

2. The deposited NH_4HSO_4 on the VTi catalyst can react with NO_x near a vanadia site on the catalyst surface. The NH_4^+ of NH_4HSO_4 can be consumed by NO, while the sulfate ion of NH_4HSO_4 remains on the catalyst surface in the form of a metal sulfate. The reaction of NH_4HSO_4 with NO_x was found as an effective way to decompose NH_4HSO_4 on the surfaces of the catalyst at low temperatures (below 300 ^oC), which indicates that accelerating this reaction can effectively restrain the continuous deposition of NH_4HSO_4 on the surfaces of the catalyst.

3. The presence of NO_2 in the feed gas significantly promotes the reaction of NH_4HSO_4 with NO_x on the catalyst surface at 250 ^oC. NO_2 was found to effectively enhance the reoxidation of V^{4+} sites, which was found to be the rate-determining step in the reaction of NH_4HSO_4 with an NO/O_2 mixture.

4. The sulfur resistance of the commercial VWTi can be significantly improved by rapidly decomposing NH_4HSO_4 on the catalyst surface using an NO/NO_2 mixture. The optimization of the reaction atmosphere could be a new strategy other than catalyst optimization to solve the sulfur poisoning problem in low-temperature SCR processes.

Acknowledgements

The financial support of National Natural Science Foundation of China (No. 51506015), Chongqing Technology Innovation and Application Demonstration Projects (cstc2018jscx-msyb0999), Fundamental Research Funds for the Central Universities (2018CDQYDL0050, 2018CDJDDL0004), and Open Fund of State Key Laboratory for Clean Energy Utilization of Zhejiang University (ZJUCEU2017016) are gratefully acknowledged.

References

[1] G. Busca, L. Lietti, G. Ramis, F. Berti, Chemical and mechanistic aspects of the selective catalytic reduction of NO_x by ammonia over oxide catalysts: A review, Appl. Catal. B: Environ., 18 (1998) 1-36.

[2] M. Bendrich, A. Scheuer, R.E. Hayes, M. Votsmeier, Unified mechanistic model for Standard SCR, Fast SCR, and NO_2 SCR over a copper chabazite catalyst, Appl. Catal. B: Environ., 222 (2018) 76-87.

[3] T. Boningari, R. Koirala, P.G. Smirniotis, Low-temperature catalytic reduction of NO by NH_3 over vanadia-based nanoparticles prepared by flame-assisted spray pyrolysis: Influence of various supports, Appl. Catal. B: Environ., 140-141 (2013) 289-298.

[4] J. Li, H. Chang, L. Ma, J. Hao, R.T. Yang, Low-temperature selective catalytic reduction of NO_x with NH_3 over metal oxide and zeolite catalysts-A review, Catal. Today, 175 (2011) 147-156.

[5] J.-K. Lai, I.E. Wachs, A Perspective on the Selective Catalytic Reduction (SCR) of NO with NH_3 by Supported V_2O_5–WO_3/TiO_2 Catalysts, ACS Catalysis, 8 (2018) 6537-6551.

[6] B. Thirupathi, P.G. Smirniotis, Nickel-doped Mn/TiO_2 as an efficient catalyst for the low-temperature SCR of NO with NH_3: Catalytic evaluation and characterizations, J. Catal., 288 (2012) 74-83.

[7] S. Deng, T. Meng, B. Xu, F. Gao, Y. Ding, L. Yu, Y. Fan, Advanced MnO_x/TiO_2 Catalyst with Preferentially Exposed Anatase {001} Facet for Low-Temperature SCR of NO, ACS Catalysis, 6 (2016) 5807-5815.

[8] P.G. Smirniotis, D.A. Peña, B.S. Uphade, Low-Temperature Selective Catalytic Reduction (SCR) of NO with NH_3 by Using Mn, Cr, and Cu Oxides Supported on Hombikat TiO_2, Angew. Chem. Int. Ed., 40 (2001) 2479-2482.

[9] Y.J. Kim, H.J. Kwon, I.-S. Nam, J.W. Choung, J.K. Kil, H.-J. Kim, M.-S. Cha, G.K. Yeo, High deNO_x performance of Mn/TiO_2 catalyst by NH_3, Catal. Today, 151 (2010) 244-250.

[10] X. Gao, X. Du, L. Cui, Y. Fu, Z. Luo, K. Cen, A Ce–Cu–Ti oxide catalyst for the selective catalytic reduction of NO with NH_3, Catal. Commun., 12 (2010) 255-258.

[11] S. Ali, L. Chen, Z. Li, T. Zhang, R. Li, S.u.H. Bakhtiar, X. Leng, F. Yuan, X. Niu, Y. Zhu, Cux-Nb1.1-x (x = 0.45, 0.35, 0.25, 0.15) bimetal oxides catalysts for the low temperature selective catalytic reduction of NO with NH_3, Appl. Catal. B: Environ., 236 (2018) 25-35.

[12] G. Yang, J. Ran, X. Du, X. Wang, Y. Chen, L. Zhang, Different copper species as active sites for NH_3-SCR reaction over Cu-SAPO-34 catalyst and reaction pathways: A periodic DFT study, Microporous Mesoporous Mater., 266 (2018) 223-231.

[13] Y. Jangjou, D. Wang, A. Kumar, J. Li, W.S. Epling, SO_2 Poisoning of the NH_3-SCR Reaction over Cu-SAPO-34: Effect of Ammonium Sulfate versus Other S-Containing Species, ACS Catalysis, 6 (2016) 6612-6622.

[14] A. Wang, P. Arora, D. Bernin, A. Kumar, K. Kamasamudram, L. Olsson, Investigation of the robust hydrothermal stability of Cu/LTA for NH_3-SCR reaction, Appl. Catal. B: Environ., 246 (2019) 242-253.

[15] Y.J. Kim, J.K. Lee, K.M. Min, S.B. Hong, I.-S. Nam, B.K. Cho, Hydrothermal stability of Cu-SSZ13 for reducing NOx by NH_3, J. Catal., 311 (2014) 447-457.

[16] T. Ryu, H. Kim, S.B. Hong, Nature of active sites in Cu-LTA NH3-SCR catalysts: A

comparative study with Cu-SSZ-13, Appl. Catal. B: Environ., 245 (2019) 513-521.
[17] X. Du, J. Xue, X. Wang, Y. Chen, J. Ran, L. Zhang, Oxidation of Sulfur Dioxide over V_2O_5/TiO_2 Catalyst with Low Vanadium Loading: A Theoretical Study, J. Phys. Chem. C, 122 (2018) 4517-4523.
[18] S.T. Choo, S.D. Yim, I.S. Nam, S.W. Ham, J.B. Lee, Effect of promoters including WO and BaO on the activity and durability of VO/sulfated TiO catalyst for NO reduction by NH, Appl. Catal. B: Environ., 44 (2003) 237-252.
[19] H. Liu, Z. Fan, C. Sun, S. Yu, S. Feng, W. Chen, D. Chen, C. Tang, F. Gao, L. Dong, Improved activity and significant SO_2 tolerance of samarium modified CeO_2-TiO_2 catalyst for NO selective catalytic reduction with NH_3, Appl. Catal. B: Environ., 244 (2019) 671-683.
[20] J. Arfaoui, A. Ghorbel, C. Petitto, G. Delahay, Novel V_2O_5-CeO_2-TiO_2-SO_4^{2-} nanostructured aerogel catalyst for the low temperature selective catalytic reduction of NO by NH_3 in excess O_2, Appl. Catal. B: Environ., 224 (2018) 264-275.
[21] H. Li, J. Zhong, H. Vehkamaki, T. Kurtén, W. Wang, M. Ge, S. Zhang, Z. Li, X. Zhang, J.S. Francisco, X.C. Zeng, Self-Catalytic Reaction of SO_3 and NH_3 to Produce Sulfamic Acid and Its Implication to Atmospheric Particle Formation, J. Am. Chem. Soc., (2018).
[22] J. Almeida, S. Schobesberger, A. Kürten, I.K. Ortega, O. Kupiainen-Määttä, A.P. Praplan, A. Adamov, A. Amorim, F. Bianchi, M. Breitenlechner, A. David, J. Dommen, N.M. Donahue, A. Downard, E. Dunne, J. Duplissy, S. Ehrhart, R.C. Flagan, A. Franchin, R. Guida, J. Hakala, A. Hansel, M. Heinritzi, H. Henschel, T. Jokinen, H. Junninen, M. Kajos, J. Kangasluoma, H. Keskinen, A. Kupc, T. Kurtén, A.N. Kvashin, A. Laaksonen, K. Lehtipalo, M. Leiminger, J. Leppä, V. Loukonen, V. Makhmutov, S. Mathot, M.J. McGrath, T. Nieminen, T. Olenius, A. Onnela, T. Petäjä, F. Riccobono, I. Riipinen, M. Rissanen, L. Rondo, T. Ruuskanen, F.D. Santos, N. Sarnela, S. Schallhart, R. Schnitzhofer, J.H. Seinfeld, M. Simon, M. Sipilä, Y. Stozhkov, F. Stratmann, A. Tomé, J. Tröstl, G. Tsagkogeorgas, P. Vaattovaara, Y. Viisanen, A. Virtanen, A. Vrtala, P.E. Wagner, E. Weingartner, H. Wex, C. Williamson, D. Wimmer, P. Ye, T. Yli-Juuti, K.S. Carslaw, M. Kulmala, J. Curtius, U. Baltensperger, D.R. Worsnop, H. Vehkamäki, J. Kirkby, Molecular understanding of sulphuric acid–amine particle nucleation in the atmosphere, Nature, 502 (2013) 359.
[23] M. Sipilä, T. Berndt, T. Petäjä, D. Brus, J. Vanhanen, F. Stratmann, J. Patokoski, R.L. Mauldin, A.-P. Hyvärinen, H. Lihavainen, M. Kulmala, The Role of Sulfuric Acid in Atmospheric Nucleation, Science, 327 (2010) 1243.
[24] Y. Shi, H. Shu, Y. Zhang, H. Fan, Y. Zhang, L. Yang, Formation and decomposition of NH_4HSO_4 during selective catalytic reduction of NO with NH_3 over V_2O_5-WO_3/TiO_2 catalysts, Fuel Process. Technol., 150 (2016) 141-147.
[25] T.K. Shlmpel Matsuda, Aklra Kato, and Fumito Nakajlma, Deposition of Ammonium Bisulfate in the Selective Catalytic Reduction of Nitrogen Oxides with Ammonia, Ind. Eng. Chem. Prod. Res. Dev., 221 (1982) 48-52.
[26] J. Menasha, D. Dunn-Rankin, L. Muzio, J. Stallings, Ammonium bisulfate formation temperature in a bench-scale single-channel air preheater, Fuel, 90 (2011) 2445-2453.
[27] L. Muzio, S. Bogseth, R. Himes, Y.-C. Chien, D. Dunn-Rankin, Ammonium bisulfate formation and reduced load SCR operation, Fuel, 206 (2017) 180-189.
[28] G. Baltin, H. Köser, K.-P. Wendlandt, Sulfuric acid formation over ammonium sulfate loaded V_2O_5–WO_3/TiO_2 catalysts by $DeNO_x$ reaction with NO_x, Catal. Today, 75 (2002) 339-

345.
[29] Z. Zhu, H. Niu, Z. Liu, S. Liu, Decomposition and Reactivity of NH_4HSO_4 on V_2O_5/AC Catalysts Used for NO Reduction with Ammonia, J. Catal., 195 (2000) 268-278.
[30] Z. Huang, Z. Zhu, Z. Liu, Q. Liu, Formation and reaction of ammonium sulfate salts on V_2O_5/AC catalyst during selective catalytic reduction of nitric oxide by ammonia at low temperatures, J. Catal., 214 (2003) 213-219.
[31] L. Song, J. Chao, Y. Fang, H. He, J. Li, W. Qiu, G. Zhang, Promotion of ceria for decomposition of ammonia bisulfate over V_2O_5-MoO_3 /TiO_2 catalyst for selective catalytic reduction, Chem. Eng. J., 303 (2016) 275-281.
[32] D. Ye, R. Qu, C. Zheng, K. Cen, X. Gao, Mechanistic investigation of enhanced reactivity of NH_4HSO_4 and NO on Nb- and Sb-doped VW/Ti SCR catalysts, Appl. Catal. A, 549 (2018) 310-319.
[33] X. Wang, X. Du, L. Zhang, Y. Chen, G. Yang, J. Ran, Promotion of NH_4HSO_4 decomposition in NO/NO_2 contained atmosphere at low temperature over V_2O_5-WO_3/TiO_2 catalyst for NO reduction, Appl. Catal. A, 559 (2018) 112-121.
[34] X. Wang, X. Du, L. Zhang, G. Yang, Y. Chen, J. Ran, Simultaneous Fast Decomposition of NH_4HSO_4 and Efficient NOx Removal by NO_2 Addition: An Option for NOx Removal in H_2O/SO_2-Contained Flue Gas at a Low Temperature, Energy & Fuels, (2018).
[35] D. Ye, R. Qu, H. Song, X. Gao, Z. Luo, M. Ni, K. Cen, New insights into the various decomposition and reactivity behaviors of NH_4HSO_4 with NO on V_2O_5/TiO_2 catalyst surfaces, Chem. Eng. J., 283 (2016) 846-854.
[36] C. Li, M. Shen, T. Yu, J. Wang, J. Wang, Y. Zhai, The mechanism of ammonium bisulfate formation and decomposition over V/WTi catalysts for NH3-selective catalytic reduction at various temperatures, Phys. Chem. Chem. Phys., 19 (2017) 15194-15206.
[37] L. Xu, C. Wang, H. Chang, Q. Wu, T. Zhang, J. Li, New Insight into SO2 Poisoning and Regeneration of CeO2–WO3/TiO2 and V2O5–WO3/TiO2 Catalysts for Low-Temperature NH3–SCR, Environmental Science & Technology, (2018).
[38] P. Li, Q. Liu, Z. Liu, Behaviors of NH_4HSO_4 in SCR of NO by NH_3 over different cokes, Chem. Eng. J., 181-182 (2012) 169-173.
[39] C. Li, M. Shen, J. Wang, J. Wang, Y. Zhai, New Insights into the Role of WO_3 in Improved Activity and Ammonium Bisulfate Resistance for NO Reduction with NH_3 over V–W/Ce/Ti Catalyst, Ind. Eng. Chem. Res., (2018).
[40] C. Li, M. Shen, J. Wang, J. Wang, Y. Zhai, New insights into the promotional mechanism of ceria for activity and ammonium bisulfate resistance over V/WTi catalyst for selective catalytic reduction of NO with NH_3, Appl. Catal. A, 560 (2018) 153-164.
[41] Z. Huang, Z. Zhu, Z. Liu, Combined effect of H_2O and SO_2 on V_2O_5/AC catalysts for NO reduction with ammonia at lower temperatures, Appl. Catal. B: Environ., 39 (2002) 361-368.
[42] Q. Yan, S. Chen, C. Zhang, Q. Wang, B. Louis, Synthesis and catalytic performance of $Cu_1Mn_{0.5}Ti_{0.5}O_x$ mixed oxide as low-temperature NH_3-SCR catalyst with enhanced SO_2 resistance, Appl. Catal. B: Environ., (2018).
[43] Y. Liu, J. Zhao, J.-M. Lee, Conventional and New Materials for Selective Catalytic Reduction (SCR) of NO_x, ChemCatChem, 10 (2018) 1499-1511.
[44] X. Wang, X. Du, L. Zhang, G. Yang, Y. Chen, J. Ran, Simultaneous Fast Decomposition of NH_4HSO_4 and Efficient NOx Removal by NO_2 Addition: An Option for NO_x Removal in

H_2O/SO_2-Contained Flue Gas at a Low Temperature, Energy & Fuels, 32 (2018) 6990-6994.
[45] D. Ye, R. Qu, H. Song, C. Zheng, X. Gao, Z. Luo, M. Ni, K. Cen, Investigation of the promotion effect of WO_3 on the decomposition and reactivity of NH_4HSO_4 with NO on V_2O_5–WO_3/TiO_2 SCR catalysts, RSC Adv., 6 (2016) 55584-55592.
[46] C. Pang, Y. Zhuo, Y. Qin, Research on the NH_4HSO_4 Decomposition Activity of Different Support-Guidance to the Development of NH_4HSO_4-Resistant SCR Catalysts for NO_x Abatement, 2018 2nd International Conference on Green Energy and Applications (ICGEA), 2018, pp. 254-262.
[47] H.H. Phil, M.P. Reddy, P.A. Kumar, L.K. Ju, J.S. Hyo, SO_2 resistant antimony promoted V_2O_5/TiO_2 catalyst for NH_3-SCR of NOx at low temperatures, Appl. Catal. B: Environ., 78 (2008) 301-308.
[48] R. Qu, D. Ye, C. Zheng, X. Gao, Z. Luo, M. Ni, K. Cen, Exploring the role of V_2O_5 in the reactivity of NH_4HSO_4 with NO on V_2O_5/TiO_2 SCR catalysts, RSC Adv., 6 (2016) 102436-102443.
[49] A.D. Becke, Density-functional exchange-energy approximation with correct asymptotic behavior, Phys. Rev. A, 38 (1988) 3098-3100.
[50] J.P. Perdew, K. Burke, M. Ernzerhof, Generalized Gradient Approximation Made Simple, Phys. Rev. Lett., 77 (1996) 3865-3868.
[51] J.K. Burdett, T. Hughbanks, G.J. Miller, J.W. Richardson, J.V. Smith, Structural-electronic relationships in inorganic solids: powder neutron diffraction studies of the rutile and anatase polymorphs of titanium dioxide at 15 and 295 K, J. Am. Chem. Soc., 109 (1987) 3639-3646.
[52] L. Arnarson, H. Falsig, S.B. Rasmussen, J.V. Lauritsen, P.G. Moses, A complete reaction mechanism for standard and fast selective catalytic reduction of nitrogen oxides on low coverage $VO_x/TiO_2(001)$ catalysts, J. Catal., 346 (2017) 188-197.
[53] L. Arnarson, H. Falsig, S.B. Rasmussen, J.V. Lauritsen, P.G. Moses, The reaction mechanism for the SCR process on monomer V(5+) sites and the effect of modified Bronsted acidity, Phys. Chem. Chem. Phys., 18 (2016) 17071-17080.
[54] C. Lee, W. Yang, R.G. Parr, Development of the Colle-Salvetti correlation-energy formula into a functional of the electron density, Physical Review B, 37 (1988) 785-789.
[55] P. Ji, X. Gao, X. Du, C. Zheng, Z. Luo, K. Cen, Relationship between the molecular structure of V_2O_5/TiO_2 catalysts and the reactivity of SO_2 oxidation, Catalysis Science & Technology, 6 (2016) 1187-1194.
[56] M.K. Hazra, A. Sinha, Formic Acid Catalyzed Hydrolysis of SO_3 in the Gas Phase: A Barrierless Mechanism for Sulfuric Acid Production of Potential Atmospheric Importance, J. Am. Chem. Soc., 133 (2011) 17444-17453.
[57] L. Li, M. Kumar, C. Zhu, J. Zhong, J.S. Francisco, X.C. Zeng, Near-Barrierless Ammonium Bisulfate Formation via a Loop-Structure Promoted Proton-Transfer Mechanism on the Surface of Water, J. Am. Chem. Soc., 138 (2016) 1816-1819.
[58] J.L. Ropero-Vega, A. Aldana-Pérez, R. Gómez, M.E. Niño-Gómez, Sulfated titania [TiO_2/SO_4^{2-}]: A very active solid acid catalyst for the esterification of free fatty acids with ethanol, Appl. Catal. A, 379 (2010) 24-29.
[59] J.P. Chen, R.T. Yang, Selective Catalytic Reduction of NO with NH_3 on SO_4^{2-}/TiO_2 Superacid Catalyst, J. Catal., 139 (1993) 277-288.
[60] S.T. Choo, S.D. Yim, I.-S. Nam, S.-W. Ham, J.-B. Lee, Effect of promoters including WO_3

and BaO on the activity and durability of V_2O_5/sulfated TiO_2 catalyst for NO reduction by NH_3, Appl. Catal. B: Environ., 44 (2003) 237-252.
[61] S.T. Choo, Y.G. Lee, I.-S. Nam, S.-W. Ham, J.-B. Lee, Characteristics of V_2O_5 supported on sulfated TiO_2 for selective catalytic reduction of NO by NH_3, Appl. Catal. A, 200 (2000) 177-188.
[62] N.-Y. Topsøe, Mechanism of the Selective Catalytic Reduction of Nitric Oxide by Ammonia Elucidated by in Situ On-Line Fourier Transform Infrared Spectroscopy, Science, 265 (1994) 1217-1219.
[63] M. Koebel, G. Madia, F. Raimondi, A. Wokaun, Enhanced Reoxidation of Vanadia by NO_2 in the Fast SCR Reaction, J. Catal., 209 (2002) 159-165.
[64] X. Wang, X. Du, G. Yang, J. Xue, Y. Chen, L. Zhang, Chemisorption of NO2 on V-Based SCR Catalysts: A Fundamental Study toward the Mechanism of "Fast SCR" Reaction, J. Phys. Chem. C, (2019) DOI: 10.1021/acs.jpcc.9b06910.
[65] X. Gao, X. Du, Y. Jiang, Y. Zhang, Z. Luo, K. Cen, A DFT study on the behavior of NO_2 in the selective catalytic reduction of nitric oxides with ammonia on a V_2O_5 catalyst surface, J. Mol. Catal. A: Chem., 317 (2010) 46-53.
[66] A. Savara, M.-J. Li, W.M.H. Sachtler, E. Weitz, Catalytic reduction of NH_4NO_3 by NO: Effects of solid acids and implications for low temperature $DeNO_x$ processes, Appl. Catal. B: Environ., 81 (2008) 251-257.